Aeolian Research 22 (2016) 85–92

Contents lists available at ScienceDirect

Aeolian Research

journal homepage: www.elsevier.com/locate/aeolia

Influence of measurement uncertainties on fractional solubility of iron in mineral aerosols over the oceans

Nicholas Meskhidze [a,*], Matthew S. Johnson [b], David Hurley [a], Kyle Dawson [a]

[a] Marine, Earth, and Atmospheric Science, North Carolina State University, Raleigh, NC, USA
[b] Earth Science Division, NASA Ames Research Center, Moffett Field, CA, USA

ARTICLE INFO

Article history:
Received 27 February 2016
Revised 10 June 2016
Accepted 13 July 2016

Keywords:
Soluble iron
Mineral dust
Measurement techniques
3-D chemical transport model

ABSTRACT

The atmospheric supply of mineral dust iron (Fe) plays a crucial role in the Earth's biogeochemical cycle and is of specific importance as a micronutrient in the marine environment. Observations show several orders of magnitude variability in the fractional solubility of Fe in mineral dust aerosols, making it hard to assess the role of mineral dust in the global ocean biogeochemical Fe cycle. In this study we compare the operational solubility of mineral dust aerosol Fe associated with the flow-through leaching protocol to the results of the global 3-D chemical transport model GEOS-Chem. According to the protocol, aerosol Fe is defined as soluble by first deionized water leaching of mineral dust through a 0.45 μm pore size membrane followed by acidification and storage of the leachate over a long period of time prior to analysis. To estimate the uncertainty in soluble Fe results introduced by the flow-through leaching protocol, we prescribe an average 50% (range of 30–70%) fractional solubility to sub-0.45 μm sized mineral dust particles that may inadvertently pass the filter and end up in the acidified (at pH ~ 1.7) leachate for a couple of month period. In the model, the fractional solubility of Fe is either explicitly calculated using a complex mineral aerosol Fe dissolution equations, or prescribed to be 1% and 4% often used by global ocean biogeochemical Fe cycle models to reproduce the broad characteristics of the presently observed ocean dissolved iron distribution. Calculations show that the fractional solubility of Fe derived through the flow-through leaching is higher compared to the model results. The largest differences (~40%) are predicted to occur farther away from the dust source regions, over the areas where sub-0.45 μm sized mineral dust particles contribute a larger fraction of the total mineral dust mass. This study suggests that different methods used in soluble Fe measurements and inconsistences in the operational definition of filterable Fe in marine environment and soluble Fe in atmospheric aerosols are likely to contribute to the wide range of fractional solubility of aerosol Fe reported in the literature.

© 2016 Elsevier B.V. All rights reserved.

1. Introduction

Earth system science models pay particular interest to interactions between ocean ecosystems and the atmosphere. These interactions have implications on trace gas exchange, bidirectional flux of particulates, and the overall global carbon budget. The improved understanding of ocean-atmosphere interaction and assessment of the ocean's role in the carbon cycle necessitates coupling of physicochemical and biological processes in the ocean. Characterization of ocean biological communities, however, requires quantitative knowledge of nutrient distribution in the Earth's oceans. Iron (Fe) is one of the crucial micronutrients in surface oceans as nearly all forms of life require sufficient amounts of Fe to carry out biological processes. Fe limitations in the oceans can be seen most readily in so-called high nitrate low chlorophyll (HNLC) waters that comprise ~30% of the global oceans (Martin and Fitzwater, 1988; Boyd et al., 2000).

Previous studies that examined the sources of new Fe (not acquired via nutrient recycling) to the oceans have largely focused on the delivery of Fe and physicochemical processes that mediate the conversion of Fe from the refractory to the soluble pool either in the surface ocean (Waite and Morel, 1984; Barbeau and Moffett, 2000) or the atmosphere (Duce et al., 1991; Meskhidze et al., 2003). Sources of new Fe to the surface ocean include upwelling and entrainment of Fe-rich waters from below the euphotic zone (Gordon et al., 1997), glacial meltwater (Smith et al., 2007; Raiswell, 2011), seasonal sea-ice retreat (Lannuzel et al., 2008), and aerosols associated with volcanism (Langmann, 2013; Hoshyaripour et al., 2014), biomass burning (Guieu et al., 2005),

* Corresponding author.
E-mail address: nmeskhidze@ncsu.edu (N. Meskhidze).

http://dx.doi.org/10.1016/j.aeolia.2016.07.002
1875-9637/© 2016 Elsevier B.V. All rights reserved.

anthropogenic emissions (Chuang et al., 2005), and mineral dust (Prospero, 1981; Duce et al., 1991; Jickells et al., 2005). Although different sources of aerosols seem to contribute to total Fe fluxes to the ocean and influence the fractional solubility of Fe in the bulk aerosol, here we only consider mineral dust. It is estimated that about 450×10^{12} g of mineral dust (Jickells et al., 2005) with an average of 3.5 weight percent of Fe (Duce and Tindale, 1991) gets deposited to the surface oceans every year. The fraction of this Fe that is in a bioavailable form and the information for the pathways that may be involved in aeolian Fe acquisition by ocean biological organisms remains the subject of active research. For example, the oversimplistic nature of the term "bioavailability" has been pointed out by Shaked and Lis (2012), suggesting that elements of Fe speciation and kinetics, phytoplankton physiology, light, temperature, and microbial interactions, are all intricately intertwined into the term bioavailability. In the marine environment greater than 99% of filterable Fe is bound to organic colloidal phases and macromolecules, usually less than 0.45 μm in size (Rue and Bruland, 1995; Barbeau, 2006; Raiswell and Canfield, 2012). So, in the ocean "filterable" or "dissolved" Fe has been operationally defined as the size fraction that passes through a 0.45 (or 0.4) μm filter membrane (Raiswell and Canfield, 2012). Since such organically-bound Fe can be taken up by phytoplankton through several known pathways (Shaked and Lis, 2012), it is considered to be bioavailable.

Because it is so difficult to quantify the bioavailability of particulate Fe in mineral dust, studies often report soluble Fe (sol-Fe) in aerosols and define this as the fraction of total Fe that contributes to the dissolved Fe inventory of surface seawater (e.g., Sholkovitz et al., 2012). However, compared to seawater, the definition of sol-Fe in mineral aerosols is less straightforward as Fe in sub-0.45 μm sized particles can contain crystalline Fe-(oxyhydr) oxides (e.g., hematite and goethite), Fe-substituted into aluminosilicate minerals, and Fe-rich nanoparticles (Claquin et al., 1999; Nickovic et al., 2013; Shi et al., 2009) that may not be readily bioavailable in seawater. Different research groups have been using a range of different leaching techniques ('batch' leaching, 'flow-through' leaching, and a combination of these two), types of Fe extraction solutions (seawater or high-purity deionized (DI) water), pH values of the solutions (from less than 2 to greater than 8), extraction times (from minutes to days), and (photo)reductant agents (oxalic, ascorbic, glyoxalic, and pyruvic acids) leading to large discrepancies in sol-Fe results (e.g., Sholkovitz et al., 2012). In addition to the range of different methods used for Fe extraction, different groups are using different operational definitions for fractional solubility of Fe in mineral dust. The sol-Fe is defined as the material that passes through a 0.2, 0.4, or 0.45 μm pore diameter filters and commonly detected through Graphite Furnace Atomic Absorption Spectroscopy (GFAAS), Inductively Coupled Plasma-Optical Emission Spectroscopy (ICP-OES), or High Resolution Inductively Coupled Plasma – Mass Spectrometry (HR-ICP-MS) (e.g., Lim and Jickells, 1990; Zhuang et al., 1990; Baker et al., 1998; Bonnet and Guieu, 2004; Mackie et al., 2006; Wu, 2007; Buck et al., 2006, 2010; Aguilar-Islas et al., 2010; Paris et al., 2011). As mentioned above, sub-0.45 μm sized particles can contain numerous different forms of Fe (both in a soluble and insoluble form), so the operational definition based on the size-sorting is bound to introduce some uncertainty in sol-Fe results. Finally, the sol-Fe portion of mineral Fe can also be defined as the sum of aqueous ferrous iron (Fe(II)) and reducible ferric (Fe(III)) iron species and measured in the solution using the hydroxylamine hydrochloride-ferrozine technique (e.g., Zhu et al., 1997; Chen and Siefert, 2004). However, such a definition is also not precise, as hydroxylamine hydrochloride can reduce ferric iron in forms ranging from aqueous to amorphous and even in some crystalline forms (Chao and Zhou, 1983; Lovley and Phillips, 1987; Verschoor and Molot, 2013).

Despite the wide variety of methods that have been used to define sol-Fe, the global-scale compilation of data carried out by Sholkovitz et al. (2012) revealed a remarkably consistent trend (similar to hyperbolic cotangent function) in the fractional solubility of aerosol Fe as a function of total aerosol Fe loading. Baker and Jickells (2006) suggested that such variability in aerosol Fe solubility is physical rather than chemical in nature, caused by preferential removal of larger mineral dust particles during atmospheric transport. Increase in surface area to volume ratio of mineral aerosol particles with transport time was proposed to yield higher solubilities (Baker and Jickells, 2006). However, using a combination of laboratory measurements of sol-Fe (in mineral dust particles with diameters from less than 0.18 to greater than 18 μm) and global aerosol model simulations, Shi et al. (2011a) showed that physical size sorting alone cannot explain observed large variability in sol-Fe values of mineral dust samples. The chemical and/or physical processing of soil dust during long-range atmospheric transport, as well as source-dependent chemical and mineralogical variations in the Fe-bearing aerosols were proposed as possible explanations for the observed variability of sol-Fe (Sholkovitz et al., 2012).

In this study using the 3-D global chemical transport model GEOS-Chem, implemented with a complex mineral dust-Fe mobilization scheme (Johnson and Meskhidze, 2013), we examine the uncertainty in Fe solubility values associated with one of the leaching techniques. The technique separates soluble and particulate forms of Fe by passing mineral dust through a 0.45 μm pore size filter, followed by acidification of the leachate and storage for a long period of time prior to the analysis (e.g., Buck et al., 2010). Using the model we first estimate the concentration of mineral dust particles with diameters less than 0.45 μm over the surface of the oceans. Then, using the reported rates for dust-Fe solubility in highly acidic solutions, we estimate the contribution of sol-Fe mobilized from these dust particles to the total measured sol-Fe. The intent of this article is in no way to criticize any of the methods used in dust Fe solubility measurements, but rather to make the reader aware of the fact that in addition to proposed physicochemical processing of soil dust during long-range atmospheric transport, the reported uncertainty in the fractional solubility of aerosol Fe is likely to be attributed to the pore diameter of the filter used for separation of soluble and particulate forms of Fe, pH of the leachate, and the time that acidified leachate is stored prior to the analysis. The priorities for future studies of the atmospheric deposition of sol-Fe to the oceans are also discussed.

2. Materials and methods

2.1. Model configuration

The global 3-D chemical transport model GEOS-Chem (v8-01-01) was applied in this study to quantify size-dependent emission rates, atmospheric concentrations, and deposition fluxes of mineral dust. The model was run with a $2 \times 2.5°$ (latitude–longitude) horizontal resolution and 47 vertical hybrid sigma-pressure levels and is driven by Goddard Earth Observing System (GEOS-5) assimilated meteorology from the NASA Global Modeling Assimilation Office (GMAO) (Bey et al., 2001). Mineral dust mobilization is calculated through the Dust Entrainment and Deposition (DEAD) scheme (Zender et al., 2003) with the source function used in the Goddard Chemistry Aerosol Radiation and Transport (GOCART) model (Ginoux et al., 2001). The detailed mineralogy of wind-blown dust from the major desert regions is prescribed using the dust

mineralogy database of Nickovic et al. (2012). Once mineral dust is mobilized from the surface, the model uses four standard dust size bins with diameter boundaries of 0.2–2.0, 2.0–3.6, 3.6–6.0 and 6.0–12.0 μm to simulate global mineral dust transport and deposition (Fairlie et al., 2007). Dry deposition in the model is based on the resistance-in-series scheme described in Wesely (1989), with the surface resistances for aerosols following the work of Zhang et al. (2001). Mineral dust removal by wet deposition processes includes both convective updraft scavenging and rainout/washout from large-scale precipitation (Liu et al., 2001). Production of sol-Fe during the atmospheric transport of mineral dust is explicitly calculated based on the chemical composition of dust at the source region, aerosol solution pH, organic (oxalate)-promoted Fe dissolution processes, and photochemical redox cycling between Fe(II) and Fe(III) (Johnson and Meskhidze, 2013). It is known that labile oxidation state of Fe in minerals can be associated with hematite, goethite, ferrihydrite, and aluminosilicates; however, for the simplicity, the hematite-based dissolution scheme is used in the current study.

2.2. Mineral dust size distribution

GEOS-Chem does not resolve explicitly mineral dust size distribution within each bin. To calculate mineral dust mass concentrations with particle diameter $D_p < 0.45$ μm [$Dust_{0.45}$], we used in situ measurements of the dust particle size distributions compiled in Mahowald et al. (2014). The solid line on Fig. 1 shows the normalized volume size distribution (V_p) as a function of dust aerosols size (D_p) using the log-log equation of $\log V_p = a \cdot \log D_p + b$, where the fit constants $a_1 = 1.71$, $a_2 = 0.89$, $b_1 = -1.47$, and $b_2 = -1.09$ were derived for the measurements with $D_p \leqslant 3$ and $D_p > 3$ μm. For the curve fitting, only the data with $D_p > 0.5$ μm (i.e., unshaded region on Fig. 1) is used, since concentration of aerosols with $D_p < 0.5$ μm may have been influenced by particles other than mineral dust (Mahowald et al., 2014). The dashed line in Fig. 1 shows the mineral dust size distribution at the emission source based on a brittle fragmentation theory from Kok (2011). To calculate [$Dust_{0.45}$] we integrated dust volume size distributions for $0.2 < D_p < 0.45$ μm and $0.2 < D_p < 2$ μm. The ratio

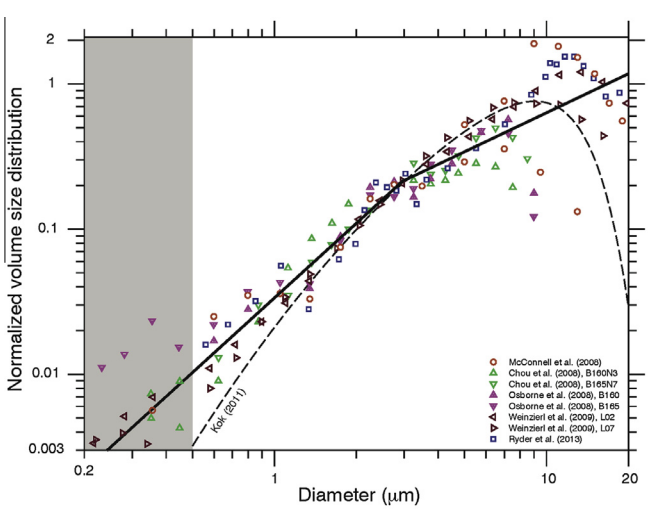

Fig. 1. In situ measurements of the dust particle size distribution close to North African source regions adapted from Mahowald et al. (2014). Solid curve shows the log-log fit used in this study. Shaded region shows data with dust particle diameter less than 0.5 μm. The measurements are from the DODO (Fig. 7 in McConnell et al., 2008), DABEX (Fig. 6 in Chou et al., 2008) and Fig. 10 in Osborne et al., 2008)), SAMUM-1 (Fig. 8 in Weinzierl et al., 2009), and Fennec (Fig. 5 in Ryder et al., 2013) field campaigns. See text for more details.

of these two volume distributions multiplied by GEOS-Chem dust mass concentration within the smallest transport bin ($0.2 < D_p < 2.0$ μm) is assumed to be equivalent to [$Dust_{0.45}$]. The difference between the Kok (2011) parameterization (applicable at the source region) and the measurements of mineral dust size distributions downwind from desert regions are thought to be attributed to differences in particle lifetime. Dust particles with $D_p > 2$ μm are more rapidly removed from the atmosphere by gravitational settling compared to ones with $D_p < 2$ μm (Shi et al., 2011a). Under identical atmospheric conditions, particles of size 1 and 10 μm will have deposition velocities 50 and 1000 times higher compared to 0.1 μm sized particles (Seinfeld and Pandis, 1998). Clouds also affect mineral dust size distribution, with in-cloud and below-cloud scavenging of mostly larger ($\geqslant 1$ μm in diameter) particles (Mahowald et al., 2014 and references therein). Although evolution of the dust size distribution towards finer sizes during transport has been reported by numerous investigators (Mahowald et al., 2014 and references therein), some current studies based on sediment traps show that particles up to 100 μm in diameter can be present at 3500 km from the African coastline (van der Does et al., 2016). Overall, when using the least square fit to the experimental data, mineral dust mass with $0.2 < D_p < 0.45$ μm represents 1.6% of dust mass within the smallest transport bin of the GEOS-Chem model ($0.2 < D_p < 2$ μm). There are caveats associated with this mineral dust mass ratio as most of the data used in Fig. 1 were collected close to North Africa sources; therefore, this ratio is expected to represent a North African dust end-member, could vary over different source regions and is likely to increase as a function of transport time.

2.3. Excess sol-Fe associated with less than 0.45 μm diameter dust particles

To determine the possible uncertainty in sol-Fe concentrations introduced by the leaching technique, we have selected a method (hereinafter called DI-Method) in which mineral dust is leached though a 0.45 μm pore size filter using high-purity DI water (pH 5.6) and subsequently acidified (typically at pH ~ 1.7) and stored (often more than several months) for offline analysis (Buck et al., 2006). The advantages of such a method are: i) the similar operational definition of sol-Fe in atmospheric aerosols as does for dissolved Fe in the ocean, and ii) the use of a rapid, flow-through leaching protocol that alleviates the potential for precipitation of Fe-hydroxides prior to collection of the leachate solution (Buck et al., 2006).

To assess the contribution of less than 0.45 μm diameter dust particles to the total measured sol-Fe, one needs to know dust-Fe solubility rates for pH ~ 1.7 hydrochloric acid (HCl) solutions over an extended period of time. Currently few studies exist that measured dissolution of mineral Fe in highly acidic media over several months. Cwiertny et al. (2008) reports an Fe solubility range of 4–16% after 24 h in a solution with pH similar to one used in the DI-Method. However, extrapolation of these values to longer times could bias our results high, as fast dissolution of Fe at the initial phase of the experiment is well documented (e.g., Shi et al., 2012). Data indicate that ~70% or more of the total Fe in aerosols collected in Bermuda is solubilized after 2 weeks storage in a solution of dilute (pH ~ 1) HCl (Kim et al., 1999; Sedwick et al., 2007). Here we use the mean value of 50% (with the range of 30–70%) for solubilization of Fe in sub-0.45 μm dust particles over a 2-month period. These values are based on the measurements of Mackie et al. (2005, 2006) and modeling studies of Ito and Xu (2014). Mackie et al. (2005, 2006) measured the release of Fe (for up to 900 h) in artificial dust (produced by abrading an Australian soil) and a natural Australian eolian dust sample taken during a dust storm. When treated with acids (pH = 1.47 and pH = 2.15),

Mackie et al. (2006) show that the release of Fe had not slowed by 600 h and can be given by the equation %sol-Fe = (0.051 ± 0.003)t + (5.6 ± 0.7) for the natural dust sample. In this equation sol-Fe is expressed in percent and t = time in hours. The Fe mobilization scheme of Ito and Xu (2014) treats three types of iron: readily released, slowly released, and refractory Fe and simulates dissolution kinetics of mineral dust under acidic conditions. Supplementary Fig. S1 shows very good agreement between measured and model predicted Fe dissolution rates for mineral dust particles.

We have carried out three model simulations. In the first model simulation we explicitly calculate sol-Fe production during the atmospheric transport of mineral dust using GEOS-Chem with explicit mineral dust-Fe mobilization scheme. In the last two simulations we prescribe 1% and 4% fractional solubility of Fe in mineral dust. Note, that the last two simulations are independent from the GEOS-Chem Fe dissolution scheme. The range in fractional solubility of Fe is the value often prescribed by global ocean biogeochemical Fe cycle models to calculate the amount of Fe that enters the ocean as bioavailable Fe (Aumont et al., 2003; Parekh et al., 2004; Tagliabue et al., 2004). All model results are then compared to the value expected from the DI-Method. The fractional enrichment in sol-Fe values (R) that would be obtained if sol-Fe concentrations in surface-level mineral dust were calculated using GEOS-Chem and the particles with $D_p \leqslant 0.45$ μm (associated with the DI-Method) were assumed to contain 50% sol-Fe:

$$R = \frac{([Dust_{tot}] - [Dust_{0.45}]) \times Fe_w \times Fe_{d2} + [Dust_{0.45}] \times Fe_w \times Fe_{d1}}{[Dust_{tot}] \times Fe_w \times Fe_{d2}} \quad (1)$$

where $[Dust_{tot}]$ and $[Dust_{0.45}]$ are the surface level (from surface to ~100 m) concentrations of mineral dust with $0.2 < D_p < 12$ μm and $0.2 < D_p < 0.45$ μm, respectively predicted by GEOS-Chem (in μg m^{-3}), Fe_w is the weight percentage of Fe in mineral dust (assumed to be 3.5%), Fe_{d1} is the fractional solubility of Fe in dust particles expected to be reached after being acidified to pH ~ 1.7 over 2-month period, and Fe_{d2} is explicitly calculated through GEOS-Chem Fe dissolution scheme or prescribed to be 1% and 4%.

3. Results

3.1. Dissolved Fe fraction in mineral dust particles

Fig. 2 shows the yearly averaged distribution of R values when GEOS-Chem model-predicted fractional solubility of Fe is used in Eq. (1). According to this figure the higher R values ~1.2–1.25 (i.e., 20–25% higher sol-Fe by the DI-Method) are expected to occur farther away from the source regions, over the areas where mineral dust particles with $D_p \leqslant 0.45$ μm contribute a larger fraction of the surface level dust mass concentration. The R values close to 1 are predicted in the vicinity of large desert regions, e.g., North African and Middle East regions, where the majority of mineral dust mass is in particles with $D_p > 1$ μm and therefore the amount of Fe mobilized in sub-0.45 μm particles (due to extended treatment of the leachate with acidic solution) will add minor amounts to total sol-Fe. Supplementary online material shows GEOS-Chem predicted yearly mean R values for Fe_{d1} of 30% and 70% (Fig. S2) and corresponding ranges in daily averaged R values (Fig. S3).

Fig. 3 shows predicted ranges in daily averaged R values over the Southern Ocean (defined here as oceanic regions south of 40°S), Equatorial Pacific (15°S-15°N, 75°W-150°W), North Atlantic Ocean (10°N-40°N, 10°W-50°W), North Pacific Ocean (40°N-80°N, 30°E-120°W) and globally for 1%, 4%, and explicitly calculated Fe solubility. This figure shows that for ambient dust-Fe solubilities the DI method can lead up to 40% overestimation of sol-Fe over the oceans, with the globally averaged R values of ~1.18 and 1.02. According to Fig. 3, the calculated R values are predicted to be highest over the Equatorial Pacific, while the North Pacific Ocean and the Southern Ocean show lower (and comparable) values.

4. Discussion

It is extremely complex to measure sol-Fe concentrations in mineral dust particles present over the oceans. However, differences in the dust source regions (i.e., mineralogy and size distribution), environmental conditions (contamination of in situ measurements by species other than mineral dust, interaction of dust particles with different acidic and organic species at variable relative humidity and temperature encountered during the atmospheric transport), sol-Fe definitions (i.e., aqueous Fe(II) and reducible Fe(III), or 0.2, 0.4, and 0.45 μm pore size filtered), and measurement methodologies (leaching procedures, chemical composition and pH values of the solutions), lead to large uncertainty in fractional solubility of Fe reported in the literature (Shi et al., 2012; Sholkovitz et al., 2012).

The DI-Method, although using a similar operational definition of sol-Fe as the dissolved Fe used in marine environments, is not consistent with the definition of bioavailable Fe in the oceans. The differences stem from the fact the sub-0.45 μm sized organically-bound Fe (the vast majority of all dissolved Fe in the oceans) can be acquired by most phytoplankton, while particulate dust-Fe in the form of crystalline Fe-(oxyhydr)oxides such as hematite and goethite, and as Fe(III) substituted into aluminosilicate minerals

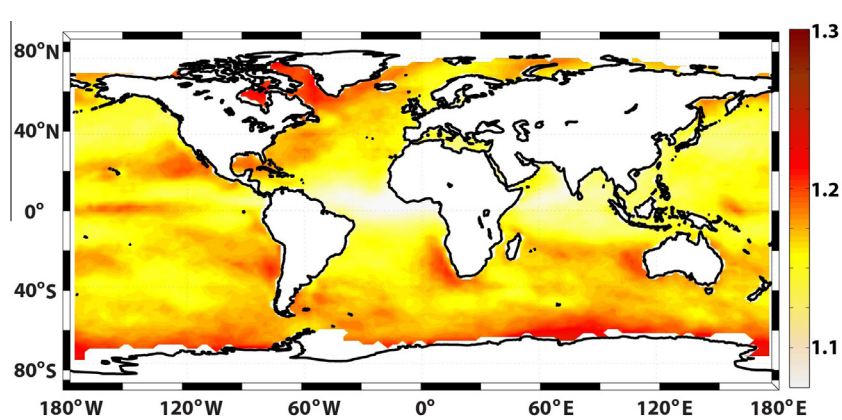

Fig. 2. GEOS-Chem-predicted annually-averaged (from March 2009 to February 2010) R values for surface-level mineral dust. Sol-Fe concentrations in mineral dust are explicitly calculated and particles with $D_p \leqslant 0.45$ μm are assumed to contain 50% sol-Fe.

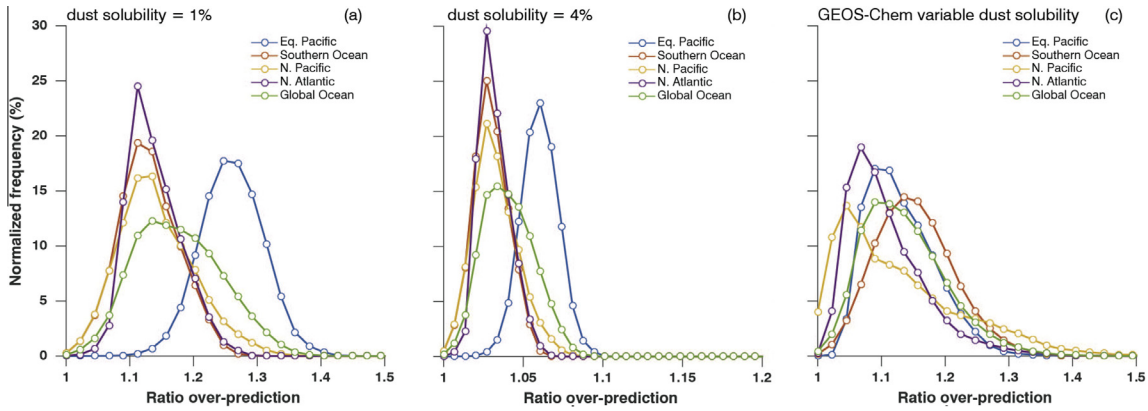

Fig. 3. GEOS-Chem-predicted normalized frequencies (%) of daily-averaged (from March 2009 to February 2010) *R* values in surface-level mineral dust when a) 1%, b) 4% of all Fe is assumed to be soluble, and c) sol-Fe fractions explicitly calculated using GEOS-Chem. The particles with $D_p \leqslant 0.45$ μm were assumed to contain 50% sol-Fe.

that could be present in sub-0.45 μm sized mineral dust is not bioavailable. To date, major ligand-complexed Fe uptake pathways have been described for phytoplankton (e.g., Shaked and Lis, 2012), while only a few organisms, e.g., the dinitrogen-fixing cyanobacterium, *Trichodesmium* spp., were shown to be capable of dissolving mineral Fe on the cell surface, and acquiring bioavailable Fe directly from mineral dust particles (Rueter et al., 1992; Rubin et al., 2011). All studies agree that long-term exposure of mineral dust samples to low pH conditions can cause sol-Fe release from the crystalline Fe pool (e.g., Mackie et al., 2005, 2006; Ito and Xu, 2014) that is not expected to be easily soluble under typical environmental conditions. Therefore, passing mineral dust through 0.45 μm sized filters followed by continued dissolution of aerosol Fe under the pH 1.7 storage conditions will likely lead to overestimations of sol-Fe values in aerosols.

To assess the possible uncertainty in sol-Fe concentrations measured using the DI-Method, we carried out GEOS-Chem model simulations in which model-predicted fractional solubility of Fe was compared to the expected Fe_{d1} from the DI-Method. If one assumes that particle morphology and Fe content does not change with size (we will come back to this point below), model simulations for annually-averaged *R* values for surface-level mineral dust reveal that overestimations in sol-Fe are trivial (i.e., $R \sim 1$) near the mineral aerosol source regions and increase (to $R \sim 1.4$) with the distance downwind as large particles are preferentially removed from the atmosphere through dry and wet deposition. In the regions where mineral dust concentration is high (i.e., above 100 μg m^{-3}), sub-0.45 μm sized mineral particles contribute less than 0.3% of total dust. Therefore when mineral dust in this small size fraction is assumed to be 50% soluble, its contribution to total fractional solubility of Fe in mineral dust samples is small. The difference between the DI-Method derived and model-predicted sol-Fe values, on the other hand, increases consistently with the distance from the mineral dust source regions. Such increase is likely associated with growing contribution of sub-0.45 μm diameter mineral particles to surface level total dust mass concentrations.

Past modeling studies have shown that chemical and physical processing of soil dust during long-range atmospheric transport can increase fractional solubility of Fe in mineral dust aerosols (Meskhidze et al., 2005; Solmon et al., 2009; Johnson et al., 2010; Shi et al., 2011a; Ito and Xu, 2014). However, in general, the magnitude is roughly a factor of 5 lower compared to the 12–15% average aerosol Fe solubility reported for high (>2 μg Fe m^{-3} air) atmospheric Fe loading of Saharan dust aerosols over the North Atlantic Ocean measured using the DI-Method (Buck et al., 2010).

So far we have only discussed the uncertainty in sol-Fe associated with a mechanism by which sub-0.45 μm size mineral dust particles, when wetted, may inadvertently pass the filter and end up in the acidified media. We suggested that over the period of months, acidic conditions (with pH ~ 1.7) could mobilize Fe from the crystal lattice of aluminosilicates, goethite, hematite, and ferrihydrite (Shi et al., 2009; Journet et al., 2008; Shi et al., 2011b; Scheuvens et al., 2011) and lead to overestimation of sol-Fe. However, due to the small contribution of sub 0.45 μm sized particles to the atmospheric mineral dust mass, such mechanism cannot explain very high Fe solubility (~20% to ~50% for Saharan dust aerosols in the $0.32 < D_p < 1.8$ and $1.8 < D_p < 3.2$ μm size ranges, respectively) reported by the measurements using the DI-Method (Buck et al., 2010). To explain these findings, we examine additional uncertainties that could be introduced by the DI-Method. Wetting can cause changes in physical size distribution (through the breakage of dust grains) and chemical composition (dissolution of salts) of mineral dust. Such changes can cause the release of additional sub-0.45 μm sized particles, finest of which are often called nanoparticles (i.e., particles with <0.1 μm in diameter). Note, that while wetting of mineral dust particles, with the subsequent breakage of dust grains, is natural and likely happens to all particles deposited through wet or dry removal to the ocean surface (high-resolution microscopy revealed the presence of Fe rich sub-0.45 particle aggregates in wet-deposited mineral dust, but did not show it in dry Saharan dust samples, Shi et al., 2009), the long-term acidification (at pH < 2) of these sub-0.45 μm sized particles involved in the DI-Method is not environmentally relevant. Therefore, the total sol-Fe measured in the leachate will be the sum of the sol-Fe extracted by the flow through technique and the additional sol-Fe associated with acid dissolution of sub-0.45 μm sized dust particles and particles that occurred due to the breakup of the dust grains.

As the abundance of sub-0.45 μm sized particles bonded to the larger dust grains or the number of sub-0.45 μm sized particles in dry mineral dust that remain aggregated due to cohesive forces change with the aerosol size distribution (Ogata et al., 2011; Baddock et al., 2013), future studies should achieve improved characterization of size-fractionated dust Fe solubility. Potential contribution from the breakup of different sized mineral dust grains to fractional solubility of Fe could be examined by measuring sol-Fe prior to and after the acidification of the leachate. Although such method for measuring size-fractionated Fe solubility could yield some insight into the differences between dust particles with variable aerodynamic diameters, it may still not be an appropriate measure for bioavailable Fe concentrations. It would be of interest to extend this recommendation to all leach protocols, particularly

ones that use a more aggressive leach medium, and to other bioactive trace elements (Shi et al., 2012).

5. Conclusions

In this study, we examined uncertainty in fractional solubility of Fe in mineral dust associated with usage of one of the flow-through leaching protocol. We argue that usage of the same operational definition of 'soluble' Fe in atmospheric aerosols as 'dissolved' Fe in seawater (i.e., passage of Fe-laden solutions through 0.45 μm pore-size filter) does not facilitate the companion of the results between different fields, as sub-0.45 μm sized mineral dust could include crystalline Fe-(oxyhydr)oxides such as hematite and goethite and Fe(III) substituted into aluminosilicate minerals that are not considered to be readily bioavailable in seawater. The long-term exposure of Fe-laden leachate solution to low pH conditions can then cause release of Fe from the pool that is not soluble under typical environmental conditions, leading to considerable overestimation of sol-Fe values of mineral dust. Our model results show that without considering changes in mineral dust size distribution due to wetting, the DI-Method derived sol-Fe can be up to 40% higher compared to the model results. The differences are particularly higher over the HNLC waters, where mineral dust particles with $D_p < 0.45$ μm can contribute higher fractions of the total surface level mineral dust mass concentration. Wetting of dry mineral dust grains during the DI-Method could lead to further uncertainties due to the physical breakage of grains, dissolution of salts and release of sub-0.45 μm sized particles that were previously bonded to each other or to the surface of larger particles. Since these particles can be highly abundant in Fe and have larger dissolution rates compared to larger Fe oxide minerals, operational solubility leaching procedure through 0.45 μm pore diameter filter can yield considerable overestimation in aerosol Fe solubility.

In terms of the wider significance, our study shows that the flow-through leaching methods that use similar operational definition of sol-Fe as the dissolved Fe in marine environments are not consistent with the definition of bioavailable Fe in the oceans. The operational definition of fractional solubility of Fe in mineral dust aerosols, as the material that passes through a 0.2, 0.4, or 0.45 μm pore diameter filter, could introduce large uncertainty in the results. Future studies should develop improved measurement techniques capable to chemically measure the speciation of Fe (in different size fractions) that are truly bioavailable in seawater.

Acknowledgements

This research was supported by NCSU Faculty Research & Professional Development Fund and the grant from the Office of Undergraduate Research at North Carolina State University. The authors would like to thank Daniel Jacob and the Harvard University Atmospheric Chemistry Modeling Group for providing the base GEOS-Chem model used during our research. Resources supporting this work were provided by the NASA High-End Computing (HEC) Program through the NASA Advanced Supercomputing (NAS) Division at NASA Ames Research Center. We also thank Dr. Akinori Ito from the Japan Agency for Marine-Earth Science and Technology (JAMSTEC) for providing the dust-Fe dissolution code used in Ito and Xu (2014).

Appendix A. Supplementary data

Supplementary data associated with this article can be found, in the online version, at http://dx.doi.org/10.1016/j.aeolia.2016.07.002.

References

Aguilar-Islas, A.M., Wu, J., Rember, R., Johansen, A.M., Shank, L.M., 2010. Dissolution of aerosol-derived iron in seawater: leach solution chemistry, aerosol type, and colloidal iron fraction. Mar. Chem. 120, 25–33. http://dx.doi.org/10.1016/j.marchem.2009.01.011.

Aumont, O., Maier-Reimer, E., Blain, S., Monfray, P., 2003. An ecosystem model of the global ocean including Fe, Si, P colimitations. Global Biogeochem. Cycles 17, 1060. http://dx.doi.org/10.1029/2001GB001745.

Baddock, M., Boskovic, L., Strong, C., McTainsh, G., Bullard, J., Agranovski, I., Cropp, R., 2013. Iron-rich nanoparticles formed by aeolian abrasion of desert dune sand. Geochem. Geophys. Geosyst. 14, 3720–3729. http://dx.doi.org/10.1002/ggge.20229.

Baker, A.R., Jickells, T.D., 2006. Mineral particle size as a control on aerosol iron solubility. Geophys. Res. Lett. 33, L17608. http://dx.doi.org/10.1029/2006GL026557.

Baker, A.R., Jickells, T.D., Witt, M., Linge, K.L., 1998. Trends in the solubility of iron, aluminium, manganese and phosphorus in aerosol collected over the Atlantic Ocean. Mar. Chem. 98, 43–58. http://dx.doi.org/10.1016/j.marchem.2005.06.004.

Barbeau, K., Moffett, J., 2000. Laboratory and field studies of colloidal iron oxide dissolution as mediated by phagotrophy and photolysis. Limnol. Oceanogr. 45, 827–835. http://dx.doi.org/10.4319/lo.2000.45.4.0827.

Barbeau, K., 2006. Photochemistry of organic iron (III) complexing ligands in oceanic systems. Photochem. Photobiol. 82, 1505–1516. http://dx.doi.org/10.1111/j.1751-1097.2006.tb09806.x.

Bey, I., Jacob, D.J., Yantosca, R.M., Logan, J.A., Field, B.D., Fiore, A.M., Li, Q., Liu, H.Y., Mickley, L.J., Schultz, M.G., 2001. Global modeling of tropospheric chemistry with assimilated meteorology: model description and evaluation. J. Geophys. Res. 106, 23073–23095. http://dx.doi.org/10.1029/2001JD000807.

Bonnet, S., Guieu, C., 2004. Dissolution of atmospheric iron in seawater. Geophys. Res. Lett. 31, L03303. http://dx.doi.org/10.1029/2003GL018423.

Boyd, P.W., Watson, A.J., Law, C.S., Abraham, E.R., Trull, T., Murdoch, R., Bakker, D.C., Bowie, A.R., Buesseler, K.O., Chang, H., Charette, M., Croot, P., Downing, K., Frew, R., Gall, M., Hadfield, M., Hall, J., Harvey, M., Jameson, G., LaRoche, J., Liddicoat, M., Ling, R., Maldonado, M.T., McKay, R.M., Nodder, S., Pickmere, S., Pridmore, R., Rintoul, S., Safi, K., Sutton, P., Strzepek, R.F., Tanneberger, K., Turner, S., Waite, A., Zeldis, J., 2000. A mesoscale phytoplankton bloom in the polar Southern Ocean stimulated by iron fertilization. Nature 315, 612–617. http://dx.doi.org/10.1038/35037500.

Buck, C.S., Landing, W.M., Resing, J.A., Lebon, G.T., 2006. Aerosol iron and aluminum solubility in the northwest Pacific Ocean: results from the 2002 IOC cruise. Geochem. Geophys. Geosyst. 7, 1–10. http://dx.doi.org/10.1029/2005GC000977.

Buck, C.S., Landing, W.M., Resing, J.A., 2010. Particle size and aerosol iron solubility: a high-resolution analysis of Atlantic aerosols. Mar. Chem. 120, 14–24. http://dx.doi.org/10.1016/j.marchem.2008.11.002.

Chao, T.T., Zhou, L., 1983. Extraction techniques for selective dissolution of amorphous iron oxides from soils and sediments. Soil Sci. Soc. Am. J. 47, 225–232.

Chen, Y., Siefert, R.L., 2004. Seasonal and spatial distributions and dry deposition fluxes of atmospheric total and labile iron over the tropical and subtropical North Atlantic Ocean. J. Geophys. Res. 109, D09305. http://dx.doi.org/10.1029/2003JD003958.

Chou, C., Formenti, P., Maille, M., Ausset, P., Helas, G., Harrison, M., Osborne, S., 2008. Size distribution, shape, and composition of mineral dust aerosols collected during the African Monsoon Multidisciplinary Analysis Special Observation Period 0: Dust and Biomass-Burning Experiment field campaign in Niger, January 2006. J. Geophys. Res. 113, D00c10.

Chuang, P.Y., Duvall, R.M., Shafer, M.M., Schauer, J.J., 2005. The origin of water soluble particulate iron in the Asian atmospheric outflow. Geophys. Res. Lett. 32, L07813. http://dx.doi.org/10.1029/2004GL021946.

Claquin, T., Schulz, M., Balkanski, Y.J., 1999. Modeling the mineralogy of atmospheric dust sources. J. Geophys. Res. 104, 22, 243–22, 256.

Cwiertny, D.M., Baltrusaitis, J., Hunter, G.J., Laskin, A., Scherer, M.M., Grassian, V.H., 2008. Characterization and acid-mobilization study of iron-containing mineral dust source materials. J. Geophys. Res. 113, D05202. http://dx.doi.org/10.1029/2007JD009332.

Duce, R.A., Tindale, N.W., 1991. Atmospheric transport of iron and its deposition in the ocean. Limnol. Oceanogr. 36, 1715–1726. http://dx.doi.org/10.4319/lo.1991.36.8.1715.

Duce, R.A., Liss, P.S., Merrill, J.T., Atlas, E.L., Buat-Menard, P., Hicks, B.B., Miller, J.M., Prospero, J.M., Arimoto, R., Church, T.M., Ellis, W., Galloway, J.N., Hansen, L., Jickells, T.D., Knap, A.H., Reinhardt, K.H., Schneider, B., Soudine, A., Tokos, J.J., Tsunogai, S., Wollast, R., Zhou, M., 1991. The atmospheric input of trace species to the world ocean. Global Biogeochem. Cycles 5, 193–259.

Fairlie, T.D., Jacob, D.J., Park, R.J., 2007. The impact of transpacific transport of mineral dust in the United States. Atmos. Environ. 41, 1251–1266. http://dx.doi.org/10.1016/j.atmosenv.2006.09.048.

Ginoux, P., Chin, M., Tegen, I., Prospero, J.M., Holben, B., Dubovik, O., Lin, S., 2001. Sources and distributions of dust aerosols simulated with the GOCART model. J. Geophys. Res. 106, 20255–20273. http://dx.doi.org/10.1029/2000JD000053.

Gordon, R.M., Coale, K.H., Johnson, K.S., 1997. Iron distributions in the equatorial Pacific: implications for new production. Limnol. Oceanogr. 42, 419–431. http://dx.doi.org/10.4319/lo.1997.42.3.0419.

Guieu, C., Bonnet, S., Wagener, T., Loÿe-Pilot, M., 2005. Biomass burning as a source of dissolved iron to the open ocean? Geophys. Res. Lett. 32, L19608. http://dx.doi.org/10.1029/2005GL022962.

Hoshyaripour, G., Hort, M., Langmann, B., Delmelle, P., 2014. Volcanic controls on ash iron solubility: new insights from high-temperature gas–ash interaction modeling. J. Volcanol. Geoth. Res. 286, 67–77. http://dx.doi.org/10.1016/j.jvolgeores.2014.09.005.

Ito, A., Xu, L., 2014. Response of acid mobilization of iron-containing mineral dust to improvement of air quality projected in the future. Atmos. Chem. Phys. 14, 3441–3459. http://dx.doi.org/10.5194/acp-14-3441-2014.

Jickells, T.D., An, Z.S., Andersen, K.K., Baker, A.R., Bergametti, G., Brooks, N., Cao, J.J., Boyd, P.W., Duce, R.A., Hunter, K.A., Kawahata, H., Kubilay, N., laRoche, J., Liss, P.S., Mahowald, N., Prospero, J.M., Ridgwell, A.J., Tegen, I., Torres, R., 2005. Global iron connections between desert dust, ocean biogeochemistry, and climate. Science 308, 67–71. http://dx.doi.org/10.1126/science.1105959.

Johnson, M., Meskhidze, N., 2013. Atmospheric dissolved iron deposition to the global oceans: effects of oxalate-promoted Fe dissolution, photochemical redox cycling, and dust mineralogy. Geosci. Model Dev. 6, 1137–1155. http://dx.doi.org/10.5194/gmd-6-1137-2013.

Johnson, M.S., Meskhidze, N., Solmon, F., Gassó, S., Chuang, P.Y., Gaiero, D.M., Yantosca, R.M., Wu, S., Wang, Y., Carouge, C., 2010. Modeling dust and soluble iron deposition to the South Atlantic Ocean. J. Geophys. Res. 115, D15202. http://dx.doi.org/10.1029/2009JD013311.

Journet, E., Desboeufs, K.V., Caquineau, S., Colin, J.L., 2008. Mineralogy as a critical factor of dust iron solubility. Geophys. Res. Lett. 35, L07805. http://dx.doi.org/10.1029/2007GL031589.

Kim, G., Alleman, L.Y., Church, T.M., 1999. Atmospheric depositional fluxes of trace elements, ^{210}Pb, and ^{7}Be to the Sargasso Sea. Global Biogeochem. Cycles 13, 1183–1192.

Kok, J.F., 2011. A scaling theory for the size distribution of emitted dust aerosols suggests climate models underestimate the size of the global dust cycle. Proc. Natl. Acad. Sci. USA 108, 1016–1021. http://dx.doi.org/10.1073/pnas.1014798108.

Langmann, B., 2013. Volcanic ash versus mineral dust: atmospheric processing and environmental and climate impacts. ISRN Atmos. Sci. 2013, 245076. http://dx.doi.org/10.1155/2013/245076.

Lannuzel, D., Schoemann, V., De Jong, J., Chou, L., Delille, B., Becquevort, S., Tison, J., 2008. Iron study during a time series in the western Weddell pack ice. Mar. Chem. 108, 85–95. http://dx.doi.org/10.1016/j.marchem.2007.10.006.

Lim, B., Jickells, T.D., 1990. Dissolved, particulate and acid-leachable trace metal concentrations in North Atlantic precipitation collected on global change expedition. Global Biogeochem. Cycles 4, 445–458.

Liu, H., Jacob, D.J., Bey, I., Yantosca, R.M., 2001. Constraints from ^{210}Pb and ^{7}Be on wet deposition and transport in a global three-dimensional chemical tracer model driven by assimilated meteorological fields. J. Geophys. Res. 106, 12109–12128. http://dx.doi.org/10.1029/2000JD900839.

Lovley, D.R., Phillips, E.J., 1987. Rapid assay for microbially reducible ferric iron in aquatic sediments. Appl. Environ. Microbiol. 53, 1536–1540.

Mackie, D.S., Boyd, P.W., Hunter, K.A., McTainsh, G.H., 2005. Simulating the cloud processing of iron in Australian dust: pH and dust concentration. Geophys. Res. Lett. 32, L06809. http://dx.doi.org/10.1029/2004GL022122.

Mackie, D.S., Peat, J.M., McTainsh, G.H., Boyd, P.W., Hunter, K.A., 2006. Soil abrasion and eolian dust production: implications for iron partitioning and solubility. Geochem. Geophys. Geosyst. 7. http://dx.doi.org/10.1029/2006GC001404, Q12Q03.

Mahowald, N., Albani, S., Kok, J.F., Engelstaeder, S., Scanza, R., Ward, D.S., Flanner, M.G., 2014. The size distribution of desert dust aerosols and its impact on the Earth system. Aeolian Res. 15, 53–71. http://dx.doi.org/10.1016/j.aeolia.2013.09.002.

Martin, J.H., Fitzwater, S., 1988. Iron deficiency limits phytoplankton growth in the north-east Pacific subarctic. Nature 331, 341–343. http://dx.doi.org/10.1038/331341A0.

Meskhidze, N., Chameides, W.L., Nenes, A., Chen, G., 2003. Iron mobilization in mineral dust: can anthropogenic SO_2 emissions affect ocean productivity? Geophys. Res. Lett. 30, 2085. http://dx.doi.org/10.1029/2003GL018035.

Meskhidze, N., Chameides, W.L., Nenes, A., 2005. Dust and pollution: a recipe for enhanced ocean fertilization? J. Geophys. Res. 110, D03301. http://dx.doi.org/10.1029/2004JD005082.

McConnell, C.L., Highwood, E.J., Coe, H., Formenti, P., Anderson, B., Osborne, S., Nava, S., Desboeufs, K., Chen, G., Harrison, M.A.J., 2008. Seasonal variations of the physical and optical characteristics of Saharan dust: results from the Dust Outflow and Deposition to the Ocean (DODO) experiment. J. Geophys. Res. 113. http://dx.doi.org/10.1029/2007JD009606, D14S05.

Nickovic, S., Vukovic, A., Vujadinovic, M., Djurdjevic, V., Pejanovic, G., 2012. Technical note: high-resolution mineralogical database of dust-productive soils for atmospheric dust modeling. Atmos. Chem. Phys. 12, 845–885. http://dx.doi.org/10.5194/acp-12-845-2012.

Nickovic, S., Vukovic, A., Vujadinovic, M., 2013. Atmospheric processing of iron carried by mineral dust. Atmos. Chem. Phys. 13, 9169–9181. http://dx.doi.org/10.5194/acp-13-9169-2013.

Ogata, H., Zhang, D., Yamada, M., Tobo, Y., 2011. Comparison of elemental composition of Asian dust particles at Amami and Amakusa during a dust event. J. Jpn. Soc. Atmos. Environ. 46, 10–19.

Osborne, S.R., Johnson, B.T., Haywood, J.M., Baran, A.J., Harrison, M.A.J., McConnell, C.L., 2008. Physical and optical properties of mineral dust aerosol during the Dust and Biomass-burning Experiment. J. Geophys. Res. 113. http://dx.doi.org/10.1029/2007JD009551, D00C03.

Parekh, P., Follows, M.J., Boyle, E., 2004. Modeling the global ocean iron cycle. Global Biogeochem. Cycles 18. http://dx.doi.org/10.1029/2003GB002061, GB1002.

Paris, R., Desboeufs, K.V., Journet, E., 2011. Variability of dust iron solubility in atmospheric waters: investigation of the role of oxalate organic complexation. Atmos. Environ. 45, 5510–5517.

Prospero, J.M., 1981. Arid regions as sources of mineral aerosols in the marine atmosphere. Geol. Soc. Am. Spec. Pap. 186, 71–86.

Raiswell, R., Canfield, D.E., 2012. The iron biogeochemical cycle past and present. Geochem. Perspect. 1, 1–214. http://dx.doi.org/10.1038/ngeo964.

Raiswell, R., 2011. Iceberg-hosted nanoparticulate Fe in the Southern Ocean: mineralogy, origin, dissolution kinetics and source of bioavailable Fe. Deep-Sea Res. II 58, 1364–1375. http://dx.doi.org/10.1016/j.dsr2.2010.11.011.

Rubin, M., Berman-Frank, I., Shaked, Y., 2011. Dust-and mineral-iron utilization by the marine dinitrogen-fixer *Trichodesmium*. Nat. Geosci. 4, 529–534. http://dx.doi.org/10.1038/ngeo1181.

Rue, E.L., Bruland, K.W., 1995. Complexation of iron (III) by natural organic ligands in the Central North Pacific as determined by a new competitive ligand equilibration/adsorptive cathodic stripping voltammetric method. Mar. Chem. 50, 117–138. http://dx.doi.org/10.1016/0304-4203(95)00031-L.

Rueter, J.G., Hutchins, D.A., Smith, R.W., Unsworth, N.L., 1992. Iron nutrition in *Trichodesmium*. In: Marine Pelagic Cyanobacteria: *Trichodesmium* and Other Diazotrophs. Springer, pp. 289–306, 362 NATO ASI Series.

Ryder, C.L., Highwood, E.J., Rosenberg, P.D., Trembath, J., Brooke, J.K., Bart, M., Dean, A., Crosier, J., Dorsey, J., Brindley, H., Banks, J., Marsham, J.H., McQuaid, J.B., Sodemann, H., Washington, R., 2013. Optical properties of Saharan dust aerosol and contribution from the coarse mode as measured during the Fennec 2011 aircraft campaign. Atmos. Chem. Phys. 13, 303–325. http://dx.doi.org/10.5194/acp-13-303-2013.

Scheuvens, D., Kandler, K., Kupper, M., Lieke, K., Zorn, S.R., Ebert, M., Schutz, L., Weinbruch, S., 2011. Individual-particle analysis of airborne dust samples collected over Morocco in 2006 during SAMUM 1. Tellus B 63, 512–530. http://dx.doi.org/10.1111/j.1600-0889.2011.00554.x.

Sedwick, P.N., Sholkovitz, E.R., Church, T.M., 2007. Impact of anthropogenic combustion emissions on the fractional solubility of aerosol iron: evidence from the Sargasso Sea. Geochem. Geophys. Geosyst. 8, Q10Q06. http://dx.doi.org/10.1029/2007GC001586.

Seinfeld, J.H., Pandis, S.N., 1998. Atmospheric Chemistry and Physics: From Air Pollution to Climate Change. John Wiley & Sons, p. 1326.

Shaked, Y., Lis, H., 2012. Disassembling iron availability to phytoplankton. Front. Microbiol. 3 (123), 1–26. http://dx.doi.org/10.3389/fmicb.2012.00123.

Shi, Z., Krom, M.D., Bonneville, S., Baker, A.R., Jickells, T.D., Benning, L.G., 2009. Formation of iron nanoparticles and increase in iron reactivity in the mineral dust during simulated cloud processing. Environ. Sci. Technol. 43, 6592–6596. http://dx.doi.org/10.1021/es901294g.

Shi, Z., Woodhouse, M., Carslaw, K., Krom, M., Baker, A., Savov, I., Mann, G., Fones, G., Brooks, B., Jickells, T., Benning, L., 2011a. Minor effect of physical size sorting on iron solubility of transported mineral dust. Atmos. Chem. Phys. 11, 8459–8469. http://dx.doi.org/10.5194/acp-11-8459-201.

Shi, Z., Bonneville, S., Krom, M., Carslaw, K., Jickells, T., Baker, A., Benning, L., 2011b. Dissolution kinetics of iron in the mineral dust at low pH during simulated atmospheric processing. Atmos. Chem. Phys. 11, 995–1007. http://dx.doi.org/10.5194/acp-11-995-2011.

Shi, Z., Krom, M.D., Jickells, T.D., Bonneville, S., Carslaw, K.S., Mihalopoulos, N., Baker, A.R., Benning, L.G., 2012. Impacts on iron solubility in the mineral dust by processes in the source region and the atmosphere: a review. Aeolian Res. 5, 21–42. http://dx.doi.org/10.1016/j.aeolia.2012.03.001.

Sholkovitz, E.R., Sedwick, P.N., Church, T.M., Baker, A.R., Powell, C.F., 2012. Fractional solubility of aerosol iron: synthesis of a global-scale data set. Geochim. Cosmochim. Acta 89, 173–189. http://dx.doi.org/10.1016/j.gca.2012.04.022.

Smith Jr., K.L., Robison, B.H., Helly, J.J., Kaufmann, R.S., Ruhl, H.A., Shaw, T.J., Twining, B.S., Vernet, M., 2007. Free-drifting icebergs: hot spots of chemical and biological enrichment in the Weddell Sea. Science 317, 478–482. http://dx.doi.org/10.1126/science.1142834.

Solmon, F., Chuang, P.Y., Meskhidze, N., Chen, Y., 2009. Acidic processing of mineral dust iron by anthropogenic compounds over the north Pacific Ocean. J. Geophys. Res. 114, D02305. http://dx.doi.org/10.1029/2008JD010417.

Tagliabue, A., Aumont, O., Bopp, L., 2004. The impact of different external sources of iron on the global carbon cycle. Geophys. Res. Lett. 41, 920–926. http://dx.doi.org/10.1002/2013GL059059.

van der Does, M., Korte, L.F., Munday, C.I., Brummer, G.-J.A., Stuut, J.-B.W., 2016. Particle size traces modern Saharan dust transport and deposition across the equatorial North Atlantic. Atmos. Chem. Phys. Discuss. 5. http://dx.doi.org/10.5194/acp-2016-344.

Verschoor, M.J., Molot, L.A., 2013. A comparison of three colorimetric methods of ferrous and total reactive iron measurement in freshwaters. Limnol. Oceanogr. Methods 11, 113–125. http://dx.doi.org/10.4319/lom.2013.11.113.

Waite, T.D., Morel, F.M., 1984. Photoreductive dissolution of colloidal iron oxides in natural waters. Environ. Sci. Technol. 18, 860–868. http://dx.doi.org/10.1021/es00129a010.

Weinzierl, B., Petzold, A., Esselborn, M., Wirth, M., Rasp, K., Kandler, K., Schutz, L., Koepke, P., Fiebig, M., 2009. Airborne measurements of dust layer properties, particle size distribution and mixing state of Saharan dust during SAMUM 2006.

Tellus B 61, 96–117. http://dx.doi.org/10.1111/j.1600-0889.2008.00392.x.
Wesely, M., 1989. Parameterization of surface resistances to gaseous dry deposition in regional-scale numerical models. Atmos. Environ. 23, 1293–1304. http://dx.doi.org/10.1016/0004-6981(89)90153-4.
Wu, J., 2007. Determination of picomolar iron in seawater by double $Mg(OH)_2$ precipitation isotope dilution high resolution ICPMS. Mar. Chem. 370–381. http://dx.doi.org/10.1016/j.marchem.2006.10.006.
Zender, C.S., Bian, H., Newman, D., 2003. Mineral Dust Entrainment and Deposition (DEAD) model: description and 1990s dust climatology. J. Geophys. Res. 108, 4416. http://dx.doi.org/10.1029/2002JD002775.
Zhang, L., Gong, S., Padro, J., Barrie, L., 2001. A size-segregated particle dry deposition scheme for an atmospheric aerosol module. Atmos. Environ. 35, 549–560. http://dx.doi.org/10.1016/S1352-2310(00)00326-5.
Zhu, X.R., Prosperoa, J.M., Millero, F.J., 1997. Diel variability of soluble Fe(II) and soluble total Fe in North African dust in the trade winds at Barbados. J. Geophys. Res. 102, 21297–21305.
Zhuang, G., Duce, R.A., Kester, D.R., 1990. The dissolution of atmospheric iron in surface seawater of the open ocean. J. Geophys. Res. Oceans 95, 16207–16216. http://dx.doi.org/10.1029/JC095iC09p16207.